Published in final edited form as:
Exp Eye Res. 2013 November ; 116: . doi:10.1016/j.exer.2013.10.006.

Pupillary Light Reflex Deficits in a Canine Model of Late Infantile Neuronal Ceroid Lipofuscinosis

Rebecca E.H. Whiting[a,b], **Kristina Narfström**[b], **Gang Yao**[a], **Jacqueline W. Pearce**[b], **Joan R. Coates**[b], **Leilani J. Castaner**[c], and **Martin L. Katz**[a,c,*]

[a]Department of Biological Engineering, University of Missouri, Columbia, MO 65211, USA

[b]Department of Veterinary Medicine and Surgery, University of Missouri, Columbia, MO 65211, USA

[c]Department of Ophthalmology, University of Missouri, Columbia, MO 65212, USA

Abstract

Late-infantile neuronal ceroid lipofuscinosis (CLN2) is a hereditary neurological disorder characterized by progressive retinal degeneration and vision loss, cognitive and motor decline, seizures, and pronounced brain atrophy. The progressive loss of neurological functions eventually leads to death, usually by the early teenage years. Utilizing a canine model of CLN2, therapeutic studies to inhibit the brain and retinal degenerations are currently under way. Using this dog model, studies were undertaken to compare quantitative assessments of the pupillary light reflex (PLR) and electroretinography (ERG) as tools for evaluating the effects of the disease on retinal function. The PLR and ERG were recorded in normal and CLN2-affected Dachshunds at 2 month intervals between the ages of 4 and 10 months. Using custom instrumentation for quantitative PLR assessments, a series of white light stimuli of varying intensity was used to elicit pupil constriction, and pupil images were recorded using continuous infrared illumination and an infrared-sensitive camera. Electroretinography was used to evaluate retinal function in the same dogs. As the disease progressed, affected dogs exhibited progressive and profound declines in ERG amplitudes under both scotopic and photopic conditions. With low intensity light stimuli, CLN2 was also accompanied by progressive deficits in the PLR. Changes in the PLR to dim light stimuli included significant deficits in latency, constriction velocity, constriction amplitude, and redilation velocity. However, despite the almost complete loss of detectable ERG responses by disease end stage, the PLR to bright stimuli was well preserved throughout the disease progression. These findings demonstrate that the PLR is much more sensitive than the ERG in detecting residual retinal function in animal models of retinal degenerative disease. The preservation of the PLR in dogs with profoundly depressed ERGs correlates with a preservation of visually-mediated behavior even late in the disease progression. Quantitative analysis of the PLR has potential as a biomarker in animal models of retinal degenerative diseases and in evaluating the efficacy of therapeutic interventions in preserving retinal function.

*Corresponding Author. University of Missouri School of Medicine, Mason Eye Institute, One Hospital Drive, Columbia, MO 65212, USA. Tel.: 01 573 882 8480; fax: 01 573 884 4100. katzm@health.missouri.edu (M.L. Katz).

Keywords

retinal degeneration; pupillary light reflex; electroretingram; neuronal ceroid lipofuscinosis; neurodegeneration; lysosomal storage disease

1. Introduction

Childhood-onset neuronal ceroid lipofuscinoses (NCLs) are autosomal recessively inherited lysosomal storage disorders characterized by progressive vision loss culminating in blindness, cognitive and motor decline, and seizures (Haltia and Goebel 2012; Mole et al. 2011). The NCLs are uniformly fatal. Clinical signs of NCL result from wide-spread, progressive neurodegeneration that is accompanied by intracellular accumulation of autofluorescent storage bodies in nervous and other tissues, including the retina (Haltia 2006). Currently, several approaches to therapy are under investigation, including gene and stem cell therapies in addition to direct enzyme replacement (Pierret et al. 2008; Hobert and Dawson 2006; Souweidane et al. 2010).

Development of effective therapeutic interventions will be facilitated by the availability of suitable animal models. Naturally-occurring NCLs have been identified in several larger animal species, including dogs (Awano et al. 2006a; Awano et al. 2006b; Bond et al. 2013; Farias et al. 2011; Katz et al. 2005; Katz et al. 2011; O'Brien and Katz 2008; Palmer et al. 2011; Sanders et al. 2010). Among the canine NCLs is a form of the disease in Dachshunds which results from a null mutation in *TPP1* that encodes the lysosomal enzyme tripeptidyl-peptidase-1 (TPP1) (Awano et al. 2006b). People with mutations in *TPP1 (CLN2)* have a form of NCL (CLN2) in which neurological signs typically first appear between 2 and 4 years of age. Affected children suffer from progressive vision loss in addition to other symptoms. The neurological decline and accompanying brain atrophy associated with CLN2 ultimately leads to death, usually by the middle teenage years (Haltia and Goebel 2012; Mole et al. 2011). Dachshunds that are homozygous for the *TPP1* null mutation develop neurological signs and vision loss similar to those observed in children with CLN2 and reach end stage disease between 10 and 11 months of age (Vuillemenot et al. 2011). The retinal pathology associated with canine CLN2 has been previously described in the Dachshund model (Katz et al. 2008). Affected dogs exhibit marked deficits in ERG b-wave amplitude by 7 months of age and significant thinning of the inner retina by disease end-stage (Katz et al. 2008).

The ERG is widely used to assess retinal function in both animals and people. It is a particularly important tool in animal studies in which it is difficult to objectively assess visual function using behavioral tests. However, the ERG only evaluates the initial portions of the pathways involved in retinal-mediated responses to light stimuli and provides no information on light-induced neurotransmission in other areas of the central nervous system (CNS). The sensitivity of the conventional ERG is also limited because of the distance between the recording electrode placed on the surface of the cornea and the retina where the ERG signals originate (Brown 1968). Consequently, subjects with profoundly depressed ERG responses can retain significant visually mediated behavior (Acland et al. 2001; Melillo et al. 2012; Narfstrom et al. 2003a; Narfstrom et al. 2003b). In addition, the PLR can be elicited with significantly dimmer stimuli than can the ERG (Whiting et al. 2013; Yao et al. 2006). Quantitative evaluation of the PLR can be used in conjunction with the ERG as a sensitive tool to evaluate the integrity of the entire complex network of neuronal circuitry involved in modulating pupil size, including the retina from which the signals that generate the PLR originate (Park et al. 2011; Fotiou et al. 2000). Utilizing the PLR in conjunction with the ERG will be particularly useful in characterizing diseases such as CLN2 in which

pathological changes occur in both the retina and other areas of the CNS involved in mediating the PLR. In these diseases, ideal therapeutic interventions would ameliorate both retinal and other CNS signs and would therefore preserve both the ERG and the PLR. In light of therapeutic studies currently under way with the Dachshund model of CLN2, studies were undertaken to determine whether the PLR is affected in this model and to assess the relationship of any changes in the PLR to disease-related ERG alterations.

2. Materials and methods

2.1. Animals

Studies employed long-haired miniature Dachshunds bred and housed in a research facility at the University of Missouri. A research colony was established by breeding from an original pair of Dachshunds that were heterozygous for a one nucleotide deletion in *TPP1* (Awano et al. 2006b). Puppies were genotyped within several weeks of birth at the *TPP1* locus using an allelic discrimination assay that distinguishes the normal and mutant alleles (Awano et al. 2006b). Most breeding consisted of carrier to carrier crosses, but periodically carrier males were bred to unrelated normal females to maintain genetic heterogeneity in the colony. Dogs utilized in this study were either homozygous normal (*TPP1* +/+) (n=14) or homozygous for the mutant allele (*TPP1* −/−) (n=9). Heterozygous carriers of the *TPP1* mutation (*TPP1* −/+) were used for breeding but were not evaluated for responses to light stimuli. Dogs were entrained to a 12:12 daily light cycle and were socialized daily in addition to receiving routine husbandry care. All studies were performed in compliance with the EU Directive 2010/63/EU for animal experiments and were approved by the University of Missouri Animal Care and Use Committee.

2.2. Ophthalmic examinations

Prior to inclusion in the study all dogs received a complete ophthalmic examination at 10–12 weeks of age, before the onset of any signs of retinal or neurological impairment due to CLN2 in the affected dogs (Katz et al. 2008). Any dogs with evidence of vision compromise or ophthalmic conditions deemed threatening to vision (n=1) were excluded from the study. Examinations were repeated monthly for CLN2-affected dogs and every other month for genetically normal dogs. Examination included visually-mediated behavioral assessment, slit lamp biomicroscopy, and indirect ophthalmoscopy. Slit lamp biomicroscopy was performed prior to dilation (SL14; Kowa Co. Ltd., Tokyo, Japan). Pupils were dilated with a short-acting mydriatic (tropicamide 1%; Alcon, Fort Worth, TX) prior to indirect ophthalmoscopy which was performed using a wireless indirect headset (12500, Welch Allyn Inc., Skaneateles Falls, NY, USA) and a handheld lens (30 diopter clear lens, Volk Optical Inc., Mentor, OH). Fundus photographs were taken following examination (NM-100; Nidek Co. Ltd., Freemont, CA) and archived electronically. Photos were reviewed to evaluate for small changes in retinal appearance.

2.3. Electroretinography

Beginning at 3 months of age, bilateral ERG evaluations were performed monthly as previously described (Katz et al. 2008). For ages at which dogs underwent PLR assessment, ERG evaluation was performed within one week after the PLR recording session. Dogs were prepared for ERG recording in ordinary room light. Prior to recording, both pupils were dilated with 1% tropicamide, and dogs were deeply sedated with intramuscular administration of dexmedetomidine (30 – 40 μg/kg). Ketamine (up to 5 mg/kg) was used in combination with the dexmedetomidine for dogs 6 months of age and younger to achieve adequate sedation. It was omitted in older dogs to reduce the risk of seizure associated with CLN2, and it was no longer necessary for adequate sedation with this age group.

ERGs were bilaterally elicited and simultaneously recorded with a portable unit (HMsERG model 2000; RetVet Corp., Columbia, MO). The right and left mini-ganzfeld domes were positioned approximately 2 cm from the corresponding eye. Each ERG session consisted of scotopic and photopic recordings in accordance with the Dog Diagnostic Protocol, recommended by the European College of Veterinary Ophthalmology, primarily for evaluation of rod and cone function (Narfström et al. 2002). Throughout a 20 minute period of dark adaptation, scotopic low-intensity rod responses were elicited at a stimulus intensity of 10.2 log photons/cm^2/s (0.01 cd/m^2) with 4 minutes of dark adaptation between recordings. Thereafter, scotopic responses were elicited using flashes of 12.65 and 13.2 log photons/cm^2/s (3 cd/m^2 and 10 cd/m^2) to evaluate mixed rod and cone function. The eyes were then exposed to diffuse white light at a luminance of 13.65 log photons/cm^2/s (30 cd/m^2) for 10 minutes, immediately after which responses to single 12.65 log photons/cm^2/s (3 cd/m^2) flash stimuli were recorded. This was immediately followed by evaluation of responses to 30-Hz photopic flicker stimuli at the same light intensity. ERG waveforms in all recordings were evaluated, and the amplitudes and implicit times for the a- and b-waves were measured as previously described (Marmor et al. 2004).

2.4. PLR recordings

The PLR was recorded in each dog at 4, 6, 8, and 10 months of age. CLN2-affected dogs were typically euthanized at 10 to 11 months of age at end-stage disease status. Uniform criteria were used for defining end-stage disease. These criteria consisted of loss of cognition, severe mentation abnormalities, loss of visual tracking, medication-refractory myoclonic jerks and inability to eat without significant assistance. The 10 month recording was not obtained in three of the affected dogs due to the need for euthanasia prior to 10 months of age. All recordings were done during the light period of the daily 12:12 light-dark cycle. The detailed methods for obtaining the PLRs have been described previously (Whiting et al. 2013). Dogs were kept in dim light (0.9 lux) for at least 1 hour, including preparation time, and in complete darkness for 10 minutes prior to recording. After 30 minutes of dim light adaptation, dogs were pre-medicated with dexmedetomidine (20–25 μg/kg IM) prior to induction of anesthesia with propofol [IV to effect, 1.49 ± 0.59 mg/kg (mean ± SD); PropoFlo 28, Abbott Laboratories, Abbott Park, IL]. Dogs were intubated with a cuffed endotracheal tube and anesthesia maintained with isoflurane (1.5% vaporizer setting; Terrell, Piramal Healthcare, Boise, ID) in oxygen. A lid speculum was inserted to ensure that the nictitating membrane and eyelids did not interfere with light exposure or visualization of the pupil. In addition, a small stay suture was placed in the bulbar conjunctiva on the central axis approximately 5 mm superior to the limbus to facilitate globe manipulation to maintain centration of the pupil on the optical axis of the recording apparatus. The eye was regularly lubricated with saline eye wash solution throughout the procedure.

Unilateral recordings were performed with a custom apparatus (Whiting et al. 2013; Fan et al. 2009) capable of timed delivery of a visible light stimulus from a mounted high-power broad spectrum LED (MCWHL2; Thorlabs Inc., Newton, NJ) and concurrent recording of pupil images at 30 frames per second using an infrared-sensitive camera (PC164CEX-2; Supercircuits Inc., Austin, TX) and continuous infrared illumination (880 nm LED) for visualization of the eye. The direct PLR of the right eye was evaluated using a standardized protocol of 100 millisecond flashes of broad spectrum white light at each of 10 intensities between 8 and 15 log photons/cm^2/s.

Pupil images were analyzed using the batch processing feature in Photoshop (Adobe Systems Inc; San Jose, CA). A list of image frame number and corresponding pupil area was exported to a spreadsheet and used to calculate desired parameters. Area measurements were

converted from pixels to mm^2 based on the known size of the lid speculum present in each pupil image.

2.5. PLR parameters

For the studies described here, baseline pupil area was the average pupil area, in a dark-adapted dog, over a 1-second period before the light stimulus. Baseline pupil diameter was calculated from area measurements assuming a round pupil. PLR constriction amplitude was defined as the difference between baseline pupil area and minimum pupil area attained following the light stimulus. These values were then converted to a percentage of baseline pupil area. Latency was defined as the time between stimulus onset and the beginning of pupil constriction. Average constriction velocity was calculated as the constriction amplitude divided by the constriction time, where constriction time is calculated between the beginning of pupil constriction and the minimum pupil size.

Redilation of the pupil is biphasic with a fast initial redilation and slower secondary redilation. Average redilation velocity was calculated for the initial redilation phase as half the constriction amplitude divided by the time required for the pupil to redilate from its minimum size to half the baseline pupil size. For the brightest flash (15 log photons/cm^2/s), the average rate of secondary redilation was calculated for the period from 15 to 85 seconds after light offset.

2.6. Statistical analysis

All statistical tests were performed using SigmaPlot (Systat Software Inc., San Jose, CA). Data were subjected to the Shapiro-Wilk test to confirm normal distribution. Repeated measures 2-way ANOVA was performed with disease status and age as the two factors. This test was used to determine if significant differences exist between the normal control group and the CLN2-affected group with respect to any of the calculated PLR or ERG parameters for a given stimulus intensity. This test also determined whether age had a significant effect on PLR parameters or if there was any significant interaction between age and disease status. Follow-up pairwise comparisons were performed with the Holm-Sidak correction (α=0.05) to control family-wise error rate. The Pearson product-moment correlation coefficient was also calculated to test for correlation amongst the PLR parameters of latency, constriction velocity, constriction amplitude, and redilation velocity.

2.7. Fluorescence Microscopy

The neuroanatomic pathway for pupillary control represents a balance between parasympathetic and sympathetic input. The CNS pathway involved in mediating the PLR in the dog includes the pretectal nuclei and the parasympathetic division of the oculomotor nuclei (Scagliotti 1999). The preganglionic neuronal cell bodies of the sympathetic neurons are located in the intermediolateral gray column of the first three thoracic spinal cord segments. Disease-related changes in neurons in these areas would be expected to affect the PLR. Therefore, analyses were performed to determine whether neurons in these areas exhibit accumulation of autofluorescent storage material that is characteristic of the NCLs similar to that which accumulates in the retinas of the affected dogs (Katz et al. 2008).

Regions of the brain and spinal cord containing the nuclei were collected shortly after euthanasia and incubated in 0.1% glutaraldehyde, 3.5% paraformaldehyde, 0.13 M sodium cacodylate, and 0.1 mM $CaCl_2$ (pH 7.4) with gentle agitation for approximately 24 hours. The samples were then incubated in 0.17 M sodium cacodylate, pH 7.4 with gentle agitation for at least 1 hour, embedded in OCT medium (Tissue-Tek; Sakura Finetek, Torrance, CA), and frozen on dry ice.

Eight-micrometer-thick sections were cut from the Tissue-Tek–embedded samples and mounted on glass slides (Super Frost; Fisher Scientific, Pittsburgh, PA) in 0.17 M sodium cacodylate. The sections were examined with a microscope (Axiophot; Carl Zeiss Meditec, Inc., Dublin, CA) equipped with epi-illumination from a high-pressure, 50-W mercury vapor lamp, a 40X objective lens (Plan-Neofluar) with a 1.3 numerical aperture, a 395- to 440-nm band-pass exciter filter, a chromatic beam splitter (FT 460), and an barrier filter (LP 515; all from Carl Zeiss Meditec, Inc.). Photography was performed with an Olympus DP72 digital camera.

3. Results

3.1. Ophthalmic exams

Initial examination in all dogs revealed normal adnexal and ocular structures. Some CLN2-affected (*TPP1* −/−) dogs developed progressive, multifocal retinal detachment lesions between the ages of 5 and 10 months (n=6) (Pearce et al. 2012). These lesions did not significantly alter the PLR or ERG except in advanced cases when affecting over 50% of the retina (Whiting REH, Pearce JW, Narfstrom K, Katz ML, in preparation, 2013). Advanced retinal lesions occurred in one affected dog at 8 months of age and in a second affected dog at 10 months of age; data obtained when these advanced lesions were present were excluded to avoid confounding factors. Other CLN2-affected dogs retained phenotypically normal fundus exams throughout the study period (n=3). Homozygous normal (*TPP1* +/+) dogs had consistently normal ophthalmic examinations throughout the study period.

3.2. ERG

The ERG a-wave was relatively well preserved in CLN2-affected dogs (Figure 1 and 2). Scotopic recordings did begin to show a decrease in a-wave amplitude at 8 months of age, and the difference between normal and affected dogs was statistically significant at 10 months of age (Figure 1 and 2A). CLN2-affected dogs exhibited substantial deficits in the b-wave amplitude of both scotopic and photopic recordings (Figure 1 and 2). Significant deficits in b-wave amplitude from rod recordings were present at 3 months of age. By 6–7 months of age, the rod response b-wave was non-recordable in affected dogs after 20 minutes of dark adaptation (Figure 2C). Scotopic recordings reflecting mixed input from rods and cones illustrated a progressive decrease in b-wave amplitude, with significant deficits beginning at 5 months of age (Figure 2D). Cone-mediated b-wave deficits were statistically significant beginning at 4 months of age and deficits continued to progress with age, though cone responses remained recordable through 10 months of age (Figure 2E). Cone inner retinal function, as illustrated by the b-wave amplitude of photopic flicker recordings, was significantly reduced in CLN2-affected dogs beginning at 5 months of age. While the deficits in flicker-induced b-wave amplitude persisted through end-stage disease, this response remained recordable through 10 months of age (Figure 2F).

3.3. PLR

No significant difference was found in baseline pupil diameter between normal dogs, 8.12 ± 0.15 mm and CLN2-affected dogs 8 months of age or younger, 8.13 ± 0.16 mm (mean ± SEM), and there was no significant change in pupil diameter with age among the normal dogs between 4 and 10 months of age. However, 10 month old CLN2-affected dogs had a significantly smaller ($p<0.01$) baseline pupil diameter than normal, 6.97 ± 0.40 mm (Figure 3). Normal dogs showed no age-related changes in any of the evaluated PLR parameters. For both normal and affected dogs, there was a significant correlation between PLR constriction amplitude and each other parameter including latency, constriction velocity, and initial redilation velocity with correlation coefficients (r) greater than 0.8 ($p<0.00001$).

PLR constriction amplitude was reduced in CLN2-affected dogs compared with that of normal dogs for stimuli between 8.5 and 13 log photons/cm^2/s (Figure 4 and 5) with data combined for dogs of all ages. For stimuli between 9 and 11 log photons/cm^2/s, constriction amplitude was already reduced from normal by 6 months of age ($p<0.03$) and further reduced at 8 months ($p<0.02$) and 10 months ($p<0.001$) of age. With a stimulus of 12 log photons/cm^2/s, constriction amplitude was significantly reduced beginning at 8 months of age. For stimuli of 8.5, 8.75, and 13 log photons/cm^2/s, the group of affected dogs as a whole was significantly reduced from the normal group with respect to constriction amplitude ($p<0.02$), but age was not a significant factor for these intensities. In addition, constriction amplitude from 10 month old CLN2-affected dogs was significantly reduced from that of 4 and 6 month old affected dogs for stimuli between 10 and 12 log photons/cm^2/s ($p<0.001$), and reduced from that of 8 month old affected dogs with a stimulus of 10 log photons/cm^2/s ($p<0.001$).

For both normal and affected dogs, PLR latency decreased as stimulus intensity increased (Figure 6). Average latency in normal dogs ranged from 320 milliseconds with a stimulus of 8.5 log photons/cm^2/s to 185 milliseconds with a stimulus of 15 log photons/cm^2/s. The PLR latency was significantly increased in 10 month old CLN2-affected dogs relative to normal dogs with stimuli between 8.75 and 11 log photons/cm^2/s ($p<0.01$). PLR latency data from 10 month old CLN2- affected dogs was significantly increased from that of 4 and 6 month old affected dogs with stimulus intensities of 9 and 10 log photons/cm^2/s ($p<0.01$).

In both normal and CLN2-affected dogs, average constriction velocity of the PLR increased with increasing stimulus intensity from 8 to 11 log photons/cm^2/s at which point it began to decrease slightly with each additional increase of stimulus intensity (Figure 7). Average constriction velocity was significantly reduced from normal in 10 month old CLN2-affected dogs with stimuli between 8.75 and 11 log photons/cm^2/s ($p<0.001$). Constriction velocity in 10 month old affected dogs was significantly reduced from that of 4, 6, and 8 month old affected dogs ($p<0.01$).

In both normal and CLN2-affected dogs, average PLR initial redilation velocity increased with increasing stimulus intensity from 8 to 11 log photons/cm^2/s at which point it began to decrease slightly with each additional increase of stimulus intensity (Figure 8). Average redilation velocities of 10 month old affected dogs were significantly reduced from normal with stimuli between 8.75 and 11 log photons/cm^2/s ($p<0.005$). Redilation velocity in 10 month old affected dogs was also significantly reduced from that of 4, 6, and 8 month old affected dogs for a stimulus of 10 log photons/cm^2/s ($p<0.05$).

Analysis of sustained pupil size after a bright stimulus (15 log photons/cm^2/s) revealed a significant delay ($p<0.025$) in secondary redilation of the pupil to baseline size in CLN2-affected dogs at 8 and 10 months of age (Figure 9). The rate of secondary redilation was significantly reduced in older affected dogs, indicating that post-illumination pupil constriction persisted longer after light offset in these dogs than in normal dogs (Figure 9).

3.4. Fluorescence Microscopy

Fluorescence microscopic examination of unstained sections of the pretectal nuclei, the parasympathetic division of the oculomotor nucleus, and the intermediolateral gray column within the first three thoracic spinal cord segments revealed substantial accumulations of autofluorescent storage material in all neurons from all three areas (Figure 10). This autofluorescent material was not present in the corresponding neurons from normal dogs.

4. Discussion

In this study we have documented clear CLN2 disease-related alterations in both the ERG, which directly measures retinal function, and the PLR, which involves central processing of signals that originate in the retina. Characterization of these deficits in the canine model will be very useful in studies to assess the efficacy of therapeutic interventions for CLN2 that are currently being evaluated for clinical use. Concurrent assessment of the ERG and PLR will be useful in the study of any disorder where functional deficits may involve either retinal or other central nervous system pathology.

At end-stage CLN2 disease, the ERG responses were either abolished or severely depressed, even with the most intense light stimuli. In contrast, while amplitudes of the PLRs elicited with low intensity stimuli decreased as the disease progressed, the PLRs to bright light stimuli remained relatively unchanged throughout the disease progression. This reflects significant preservation of retinal function and of the neural pathways involved in the PLR. This also supports the idea that the PLR is more sensitive than the ERG in detecting residual retinal function in retinal degenerative disorders, even in cases such as CLN2 where pathology in the central PLR neural pathway may occur. This is consistent with our previous finding that in normal dogs the stimulus intensity required to elicit a threshold PLR is approximately 10-fold lower than that required to elicit a scotopic threshold ERG response in the dark-adapted state (Whiting et al. 2013).

CLN2 results from the absence of or deficiency in tripeptidyl pepetidase-1 (TPP1), a soluble lysosomal enzyme that can be taken up by cells after binding to cell-surface receptors and then transported to lysosomes via the endosomal system (Kyttälä et al. 2006). Therefore, like similar lysosomal storage disorders, CLN2 may be treatable with enzyme replacement therapy (ERT) (Vuillemenot et al. 2011). In a recent study, we found that long-term periodic infusion of recombinant TPP1 into the cerebrospinal fluid of affected dogs delayed the progression of neurological signs and brain atrophy, but did not alter the progressive decline in the ERG, which eventually became non-recordable under any stimulus condition (Whiting et al., in preparation). Behaviorally these dogs appeared to retain useful vision even after no ERG responses could be elicited. Thus, as demonstrated in previous studies (Bainbridge et al. 2008; Williams and Jacobs 2007), the absence of a recordable ERG does not necessarily mean than an animal has lost all visual function. The data from the current study suggest that the PLR may be more useful in detecting residual retinal function in some situations. Indeed, human patients treated with RPE gene replacement therapy for Leber congenital amaurosis exhibited a long-term restoration of the PLR and visual function in the absence of recordable ERG responses (Testa et al. 2013).

Because the neural pathways involved in mediating the PLR and visual perception diverge, preservation or restoration of the PLR and of visual function may not always correlate. In most human subjects, establishing such a correlation is relatively easy due to many available methods for assessing visual perception. In animal models, assessment of visual perception is much more difficult, so particularly in models of diseases such as CLN2 that affect both the retina and the central nervous system, the ERG is still an important tool despite its limited sensitivity. The ideal goal of therapies for retinal degenerative disorders is to restore or preserve as much retinal function as possible, so to be more than moderately successful these therapies should result not only in detectable PLR responses, but in at least partial restoration or preservation of the ERG.

Changes in the PLR of CLN2-affected dogs were observed with dim stimuli, including significant deficits in constriction amplitude, latency, constriction velocity, and initial redilation velocity which all depend largely on input from the parasympathetic system.

Given the strong correlation between constriction amplitude and these other parameters, deficits in all parameters are likely tied to one another and indicate reduced parasympathetic input to the PLR. The stimulus intensities with which deficits were observed are below the threshold of melanopsin input indicating that the PLR response with these stimuli would be mainly driven by the rod/cone input (Lucas et al. 2003). Lall et. al. found that in mice cone input dominates the PLR with dim stimuli, while intrinsic melanopsin input dominates the PLR with greater intensity stimuli (Lall et al. 2010). Preservation of the PLR and the sustained constriction to bright stimuli suggests that the photosensitive ganglion cells containing melanopsin remain functionally intact in CLN2.

CLN2-affected dogs also exhibited delays in the secondary redilation phase of the PLR and a reduction in baseline pupil size. Each of these findings may point to a deficit in sympathetic input to the PLR or a deficit in fibers that inhibit the parasympathetic division of the oculomotor nucleus (equivalent to the human Edinger Westphal nucleus) (Heller et al. 1990). Baseline pupil size is mediated by the sympathetic and parasympathetic innervations of the iris sphincter and dilator muscles. Therefore, in order for the baseline pupil to be more constricted, the ratio of sympathetic input that promotes dilation to the parasympathetic input that promotes constriction must be reduced. In addition to direct sympathetic and parasympathetic input to the PLR, central inhibition of the parasympathetic system also plays a role in regulating this balance (Heller et al. 1990).

The disease-related accumulation of autofluorescent storage material in the midbrain and spinal cord neurons involved in the PLR support a role for CNS changes in the disease-related alterations in PLR responses. The substantial build-up of this material could result in impaired cell function. It is possible that the observed reduction in PLR amplitudes to low intensity stimuli, even early in the disease process, may have been due at least in part to functional impairment in these interneurons as well as to reduced input from the retina.

The characterization of disease-related alterations in light induced responses contributes to our understanding of the pathology underlying CLN2. Preventing development of the deficits in the PLR and ERG responses can be used to objectively assess the efficacy of therapeutic interventions for CLN2 that are currently under development. An ideal therapy would prevent the declines in both the PLR and the ERG responses by preventing both retina and brain degeneration.

Acknowledgments

The authors thank Drs. Christine Sibigtroth and Melissa Carpentier for assistance with anesthesia. We also thank Dr. Gayle C. Johnson for her assistance with necropsies.

Disclosure statement, funding and role of funding source

Thus study was supported by grant EY018815 from the U.S. National Institutes of Health, and by grants from the Batten Disease Support and Research Association, the University of Missouri Research Board and the University of Missouri Mizzou Advantage program. These sponsors were not involved in the study design, the collection, analysis and interpretation of the data, the writing of this report, or in the decision to submit the article for publication.

References

Acland G, Aguirre G, Ray J, Zhang Q, Aleman T, Cideciyan A, Pearce-Kelling S, Anand V, Zeng Y, Maguire A, Jacobson S, Hauswirth W, Bennett J. Gene therapy restores vision in a canine model of childhood blindness. Nat Genet. 2001; 28:92–5. [PubMed: 11326284]

Awano T, Katz M, O'Brien D, Taylor J, Evans J, Khan S, Lobel P, Sohar I, Johnson G. A mutation in the cathepsin D gene (CTSD) in American Bulldogs with neuronal ceroid-lipofuscinosis. Molec Genet Metab. 2006a; 87:341–8. [PubMed: 16386934]

Awano T, Katz ML, O'Brien DP, Sohar I, Lobel P, Coates JR, Khan S, Johnson GC, Giger U, Johnson GS. A frame shift mutation in canine TPP1 (the ortholog of human CLN2) in a juvenile Dachshund with neuronal ceroid lipofuscinosis. Molec Genet Metab. 2006b; 89:254–60. [PubMed: 16621647]

Bainbridge JWB, Smith AJ, Barker SS, Robbie S, Henderson R, Balaggan K, Viswanathan A, Holder GE, Stockman A, Tyler N, Petersen-Jones S, Bhattacharya SS, Thrasher AJ, Fitzke FW, Carter BJ, Rubin GS, Moore AT, Ali RR. Effect of Gene Therapy on Visual Function in Leber's Congenital Amaurosis. N Engl J Med. 2008; 358:2231–9. [PubMed: 18441371]

Bond M, Holthaus S-MK, Tammen I, Tear G, Russell C. Use of model organisms for the study of neuronal ceroid lipofuscinosis. Biochim Biophys Acta. 2013; 1832:1842–65. [PubMed: 23338040]

Brown KT. The electroretinogram: its components and their origins. Vision Res. 1968; 8:633–77. [PubMed: 4978009]

Fan X, Miles JH, Takahashi N, Yao G. Sex-Specific Lateralization of Contraction Anisocoria in Transient Pupillary Light Reflex. Invest Ophthalmol Vis Sci. 2009; 50:1137–44. [PubMed: 18836163]

Farias FH, Zeng R, Johnson GS, Wininger FA, Taylor JF, Schnabel RD, McKay SD, Lohi H, Lindblad-Toh K, Wade C, O'Brien DP, Katz ML. A truncating mutation in ATP13A2 is responsible for adult-onset neuronal ceroid lipofuscinosis in Tibetan Terriers. Neurobiol Dis. 2011; 42:468–74. [PubMed: 21362476]

Fotiou F, Fountoulakis KN, Goulas A, Alexopoulos L, Palikaras A. Automated standardized pupillometry with optical method for purposes of clinical practice and research. Clin Physiol. 2000; 20:336–47. [PubMed: 10971544]

Haltia M. The neuronal ceroid-lipofuscinoses: From past to present. Biochim Biophys Acta. 2006; 1762:850–856. [PubMed: 16908122]

Haltia M, Goebel HH. The neuronal ceroid-lipofuscinoses: A historical introduction. Biochim Biophys Acta Elsevier BV. 2012; 1832:1795–800.

Heller PH, Perry F, Jewerr L, Levinef JD. Autonomic Components of the Human Pupillary Light Reflex. Invest Ophthalmol Vis Sci. 1990; 31(1)

Hobert JA, Dawson G. Neuronal ceroid lipofuscinoses therapeutic strategies: Past, present and future. Biochim Biophys Acta. 2006; 1762:945–953. [PubMed: 17049436]

Katz M, Coates J, Cooper J, O'Brien DP, Jeong M, Narfstrom K. Retinal Pathology in a Canine Model of Late Infantile Neuronal Ceroid Lipofuscinosis. Invest Ophthalmol Vis Sci. 2008; 49:2686–95. [PubMed: 18344450]

Katz M, Khan S, Awano T, Shahid A, Siakotos A, Johnson G. A mutation in the CLN8 gene in English Setter dogs with neuronal ceroid lipofuscinosis. Biochem Biophys Res Commun. 2005; 327:541–7. [PubMed: 15629147]

Katz ML, Farias FH, Sanders DN, Zeng R, Khan S, Johnson GS, O'Brien DP. A missense mutation in canine CLN6 in an Australian shepherd with neuronal ceroid lipofuscinosis. J biomed biotechnol. 2011; 2011:1–6.

Kyttälä A, Lahtinen U, Braulke T, Hofmann SL. Functional biology of the neuronal ceroid lipofuscinoses (NCL) proteins. Biochim Biophys Acta. 2006; 1762:920–933. [PubMed: 16839750]

Lall GS, Revell VL, Momiji H, AlEnezi J, Altimus CM, Gu AD, Aguilar C, Cameron MA, Allender S, Hankins MW, Lucas RJ. Distinct Contributions of Rod, Cone, and Melanopsin Photoreceptors to Encoding Irradiance. Neuron. 2010; 66:417–28. [PubMed: 20471354]

Lucas RJ, Hattar S, Takao M, Berson DM. Diminished Pupillary Light Reflex at High Irradiances in Melanopsin-Knockout Mice. Science. 2003; 299:245–7. [PubMed: 12522249]

Marmor MF, Holder GE, Seeliger MW, Yamamoto S. Standard for clinical electroretinography (2004 update). Doc Ophthalmol. 2004; 108:107–14. [PubMed: 15455793]

Melillo P, Pecchia L, Testa F, Rossi S, Bennett J, Simonelli F. Pupillometric analysis for assessment of gene therapy in Leber Congenital Amaurosis patients. Biomed Eng Online. 2012; 11:40. [PubMed: 22812667]

Mole, SE.; Williams, RE.; Goebel, HH. The Neuronal Ceroid Lipofuscinoses (Batten Disease). 2. London: Oxford University Press; 2011.

Narfström K, Ekesten B, Rosolen SG, Spiess BM, Percicot CL, Ofri R. Guidelines for clinical electroretinography in the dog. Doc Ophthalmol. 2002; 105:83–92. [PubMed: 12462438]

Narfstrom K, Katz M, Ford M, Redmond T, Rakoczy E, Bragadottir R. In Vivo Gene Therapy in Young and Adult RPE65−/− Dogs Produces Long-Term Visual Improvement. J Hered. 2003a; 94:31–7. [PubMed: 12692160]

Narfstrom K, Katz ML, Bragadottir R, Seeliger M, Boulanger A, Redmond TM, Caro L, Lai C, Rakoczy PE. Functional and Structural Recovery of the Retina after Gene Therapy in the RPE65 Null Mutation Dog. Invest Ophthalmol Vis Sci. 2003b; 44:1663–72. [PubMed: 12657607]

O'Brien DP, Katz ML. Neuronal ceroid lipofuscinosis in three Australian shepherd littermates. J Vet Intern Med. 2008; 22:472–5. [PubMed: 18371036]

Palmer, D.; Tammen, I.; Drogemuller, C.; Johnson, G.; Katz, M.; Lingaas, F. Large animal models of neuronal ceroid lipofuscinoses. In: Mole, S.; Williams, R.; Goebel, H., editors. The Neuronal Ceroid Lipofuscinoses (Batten Disease). 2. London: Oxford University Press; 2011. p. 284-320.

Park JC, Moura AL, Raza AS, Rhee DW, Kardon RH, Hood DC. Toward a Clinical Protocol for Assessing Rod, Cone, and Melanopsin Contributions to the Human Pupil Response. Invest Ophthalmol Vis Sci. 2011; 52:6624–35. [PubMed: 21743008]

Pearce JW, Whiting REH, Castaner L, Narfström K, Katz ML. Multifocal Retinopathy in A Colony of Miniature Longhaired Dachshunds with Late Infantile Neuronal Ceroid Lipofuscinosis. 43rd Annual Meeting of the American College of Veterinary Ophthalmologists. 2012

Pierret C, Morrison JA, Kirk MD. Treatment of lysosomal storage disorders: Focus on the neuronal ceroid-lipofuscinoses. Acta Neurobiol Exp (Warsz). 2008; 68:429–42. [PubMed: 18668166]

Sanders DN, Farias FH, Johnson GS, Chiang V, Cook JR, O'Brien DP, Hofmann SL, Lu J-Y, Katz ML. A mutation in canine PPT1 causes early onset neuronal ceroid lipofuscinosis in a Dachshund. Mol Genet Metab. 2010; 100:349–56. [PubMed: 20494602]

Scagliotti, RH. Comparative Neuro-ophthalmology. In: Gellat, KN., editor. Vet Ophthalmol. 3. Gainesville, FL: Lippincott Williams & Wilkins; 1999. p. 1307-400.

Souweidane MM, Fraser JF, Arkin LM, Sondhi D, Hackett NR, Kaminsky SM, Heier L, Kosofsky BE, Worgall S, Crystal RG, Kaplitt MG. Gene therapy for late infantile neuronal ceroid lipofuscinosis: neurosurgical considerations. J Neurosurg Pediatrics. 2010; 6:115–22.

Testa F, Maguire AM, Rossi S, Pierce EA, Melillo P, Marshall K, Banfi S, Surace EM, Sun J, Acerra C, Wright JF, Wellman J, High KA, Auricchio A, Bennett J, Simonelli F. Three-Year Follow-up after Unilateral Subretinal Delivery of Adeno-Associated Virus in Patients with Leber Congenital Amaurosis Type 2. Ophthalmology. 2013; 120:1283–91. [PubMed: 23474247]

Vuillemenot BR, Katz ML, Coates JR, Kennedy D, Tiger P, Kanazono S, Lobel P, Sohar I, Xu S, Cahayag R, Keve S, Koren E, Bunting S, Tsuruda LS, O'Neill Ca. Intrathecal tripeptidyl-peptidase 1 reduces lysosomal storage in a canine model of late infantile neuronal ceroid lipofuscinosis. Molec Genet Metab. 2011; 104:325–37. [PubMed: 21784683]

Whiting REH, Yao G, Narfström K, Pearce JW, Coates JR, Dodam JR, Castaner LJ, Katz ML. Quantitative Assessment of the Canine Pupillary Light Reflex. Invest Ophthalmol Vis Sci. 2013; 54:5432–40. [PubMed: 23847311]

Williams GA, Jacobs GH. Cone-based vision in the aging mouse. Vision Research. 2007; 47:2037–46. [PubMed: 17509638]

Yao G, Zhang K, Bellassai M, Chang B, Lei B. Ultraviolet Light – Induced and Green Light – Induced Transient Pupillary Light Reflex in Mice. Curr Eye Res. 2006; 31:925–33. [PubMed: 17114118]

Highlights

- Electroretinogram and pupillary light reflex were evaluated in dogs with retinal degeneration.
- Pupillary light reflexes were better preserved than electroretinogram responses.
- Pupillary light reflex measurements are a sensitive measure of retinal functional integrity.

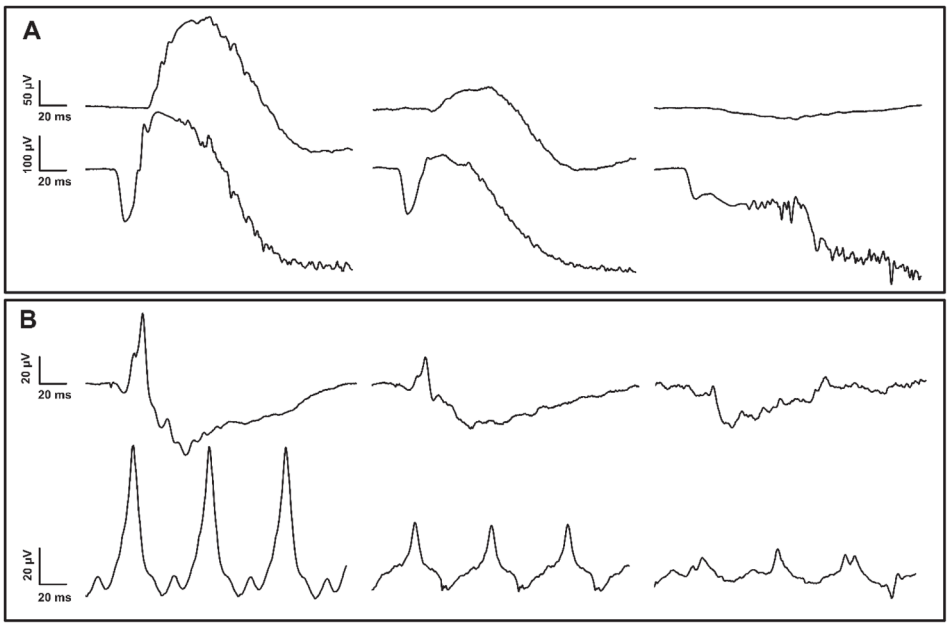

Figure 1.

Representative ERG tracings from a 10 month old normal dog (left), 6 month old affected dog (middle) and 10 month old affected dog (right). (A) Scotopic rod recordings (top) and 10 cd.s/m^2 mixed rod and cone recordings (bottom). (B) Photopic cone single flash (top) and 30 Hz flicker recordings (bottom).

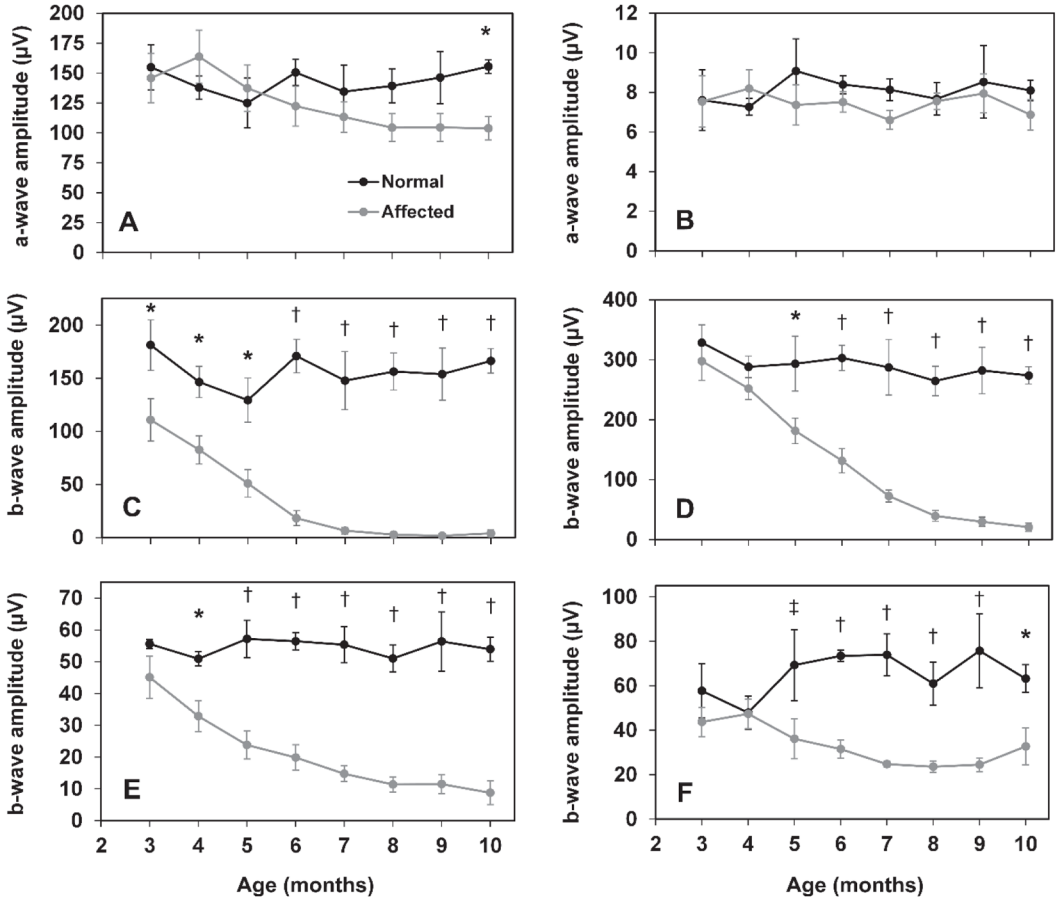

Figure 2.

ERG amplitudes as a function of age in normal and CLN2-affected dogs. ERG a-wave amplitude from 10 cd.s/m^2 scotopic (A), and 3 cd.s/m^2 photopic (B) recordings. Significant deficits in a-wave amplitude are not present until 10 months of age and only with scotopic recordings. ERG b-wave amplitude from scotopic rod responses (C), scotopic mixed responses from rods and cones at 10 cd.s/m^2 (D), and photopic cone (E) and 30 Hz flicker recordings (F). Significant differences in b-wave amplitude exist even in early stages of disease (†, $p<0.001$; *, $p<0.005$; ‡, $p<0.05$). Error bars represent SEM.

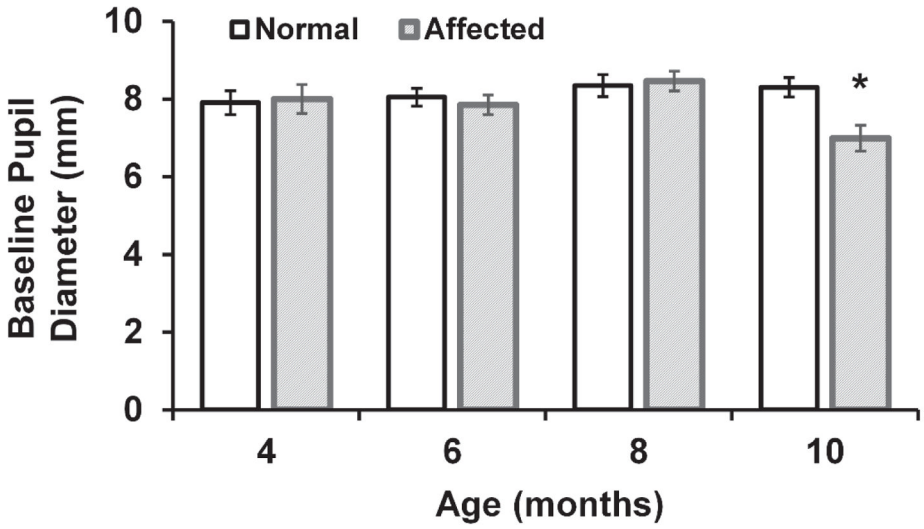

Figure 3.

Baseline pupil diameter in anesthetized normal and CLN2-affected dogs between 4 and 10 months of age. Baseline diameter is significantly reduced in 10 month old affected dogs compared to 10 month old normal dogs (*, $p<0.01$). Due to the development of severe retinal lesions and euthanasia prior to 10 months of age for some dogs, sample size for the CLN2-affected group was reduced at 8 months (n=8) and 10 months (n=5) of age.

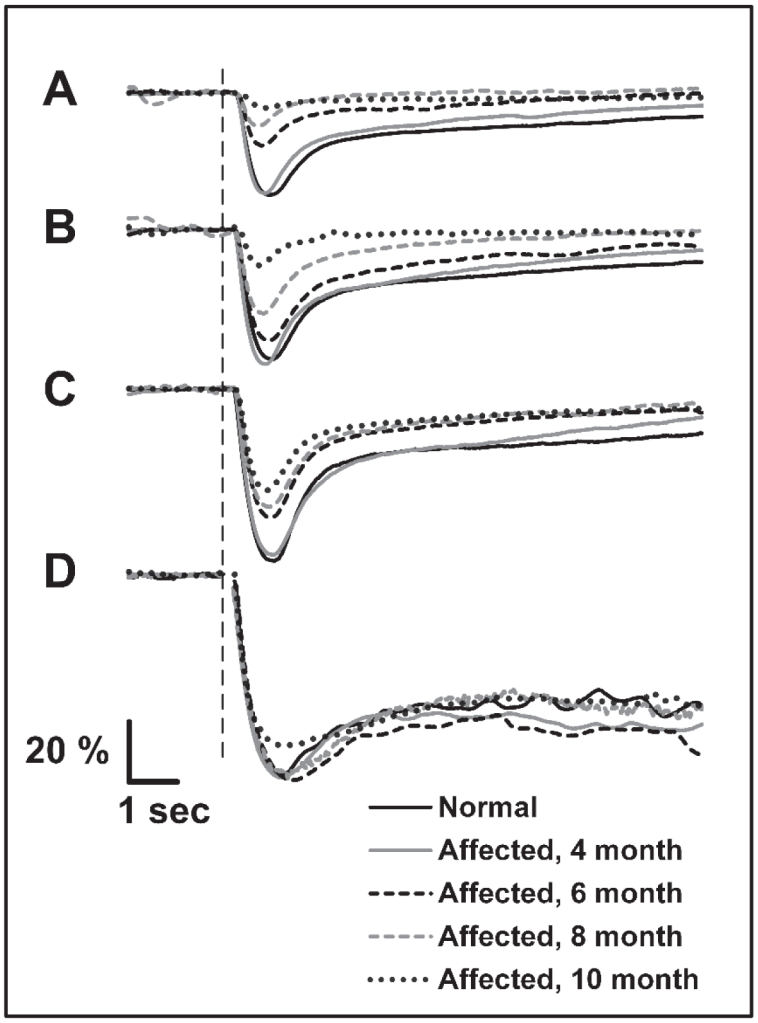

Figure 4.

Representative PLR traces from a normal dog at 10 months of age and a CLN2-affected dog between 4 and 10 months of age. Pupil responses are shown as percent of baseline pupil area. PLRs are in response to stimuli of 9, 10, 11, and 15 log photons/cm^2/s (AD, respectively). The vertical dashed line represents stimulus onset.

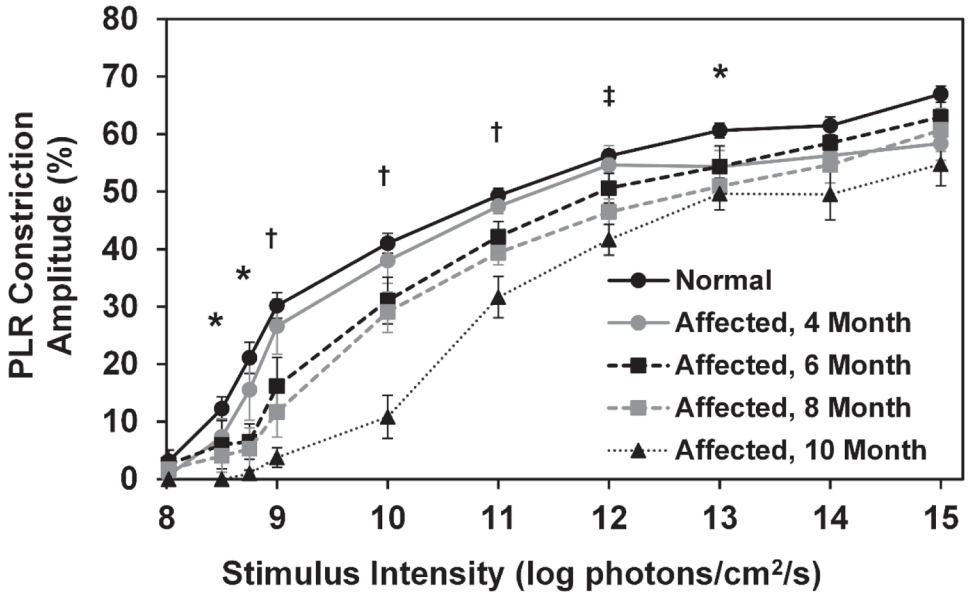

Figure 5.

PLR constriction amplitude as a function of stimulus intensity in normal and CLN2-affected dogs. Amplitudes from normal dogs include combined data from dogs of all ages examined. For stimulus intensities between 9 and 11 log photons/cm^2/s, constriction amplitude of affected dogs was progressively reduced from normal; differences were significant beginning at 6 months of age (†, $p<0.03$). With a stimulus of 12 log photons/cm^2/s, constriction amplitude was not significantly reduced until 8 months of age (‡, $p<0.02$). Age was not a significant factor for stimuli of 8.5, 8.75, and 13 log photons/cm^2/s, but constriction amplitude of the CLN2-affected group as a whole was significantly reduced from normal (*,$p<0.02$). Error bars represent SEM.

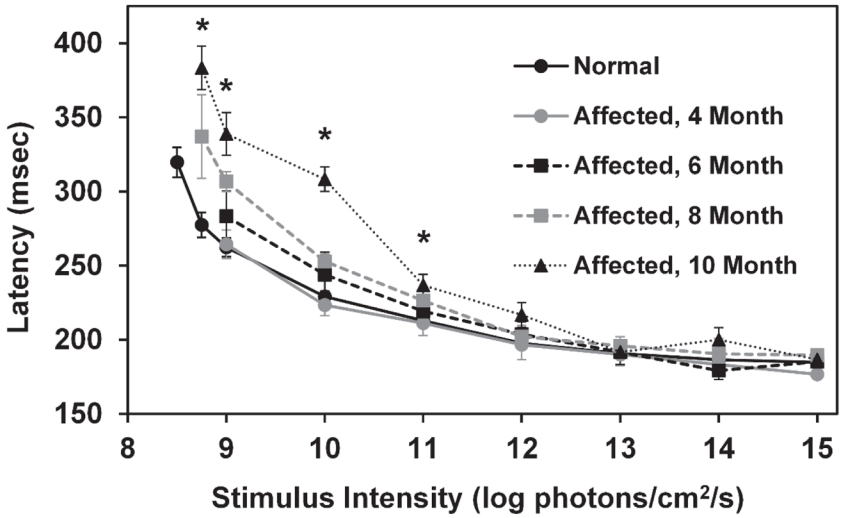

Figure 6.

PLR latency as a function of stimulus intensity. Latency is significantly longer in CLN2-affected dogs at 10 months of age for stimuli between 8.75 and 11 log photons/cm^2/s (*, $p<0.01$). In addition, the increase in PLR latency was significantly greater in the 10 month old CLN2-affected dogs compared with 4 and 6 month old dogs for stimuli of 9 and 10 log photons/cm^2/s. Error bars represent SEM.

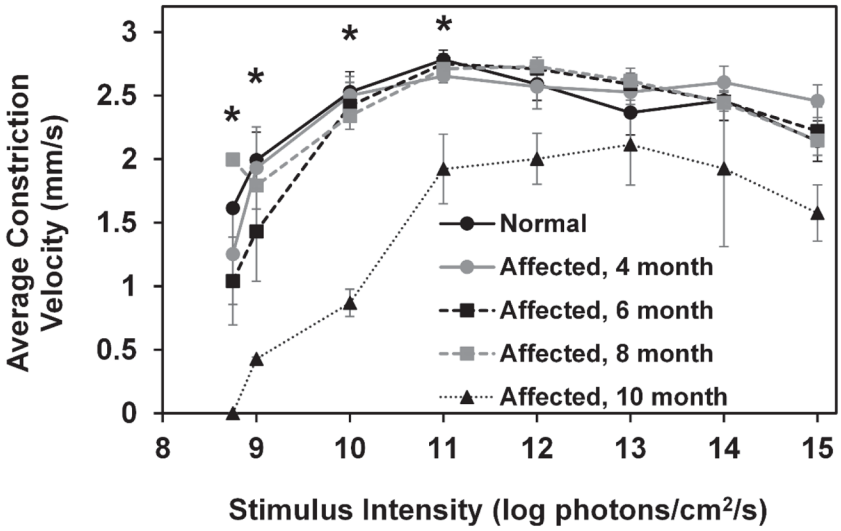

Figure 7.

Average constriction velocity was significantly reduced in 10 month old CLN2-affected dogs with stimuli between 8.75 and 11 log photons/cm^2/s (*,$p<0.001$). Error bars represent SEM.

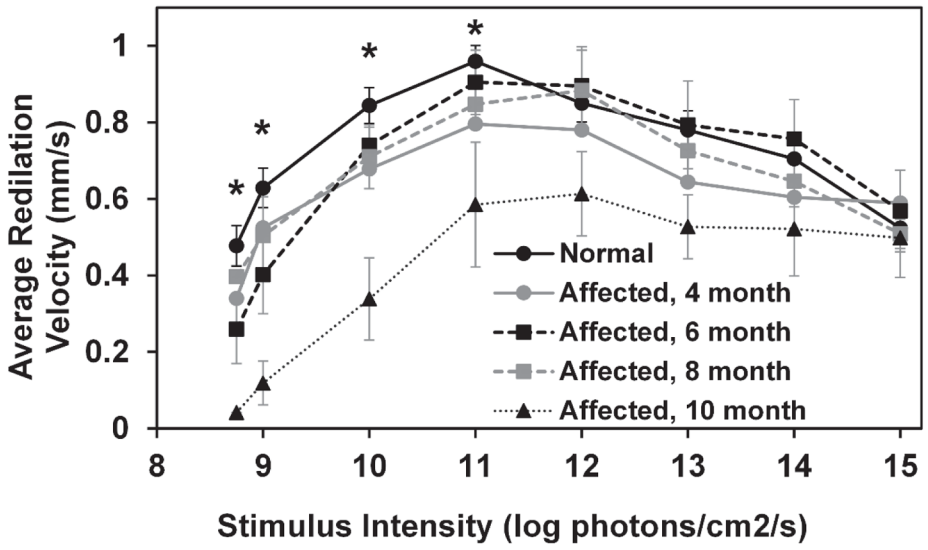

Figure 8.

Average redilation velocity as a function of stimulus intensity. Redilation velocity is significantly reduced in 10 month old CLN2-affected dogs with stimuli between 8.75 and 11 log photons/cm^2/s (*, $p<0.005$). Error bars represent SEM.

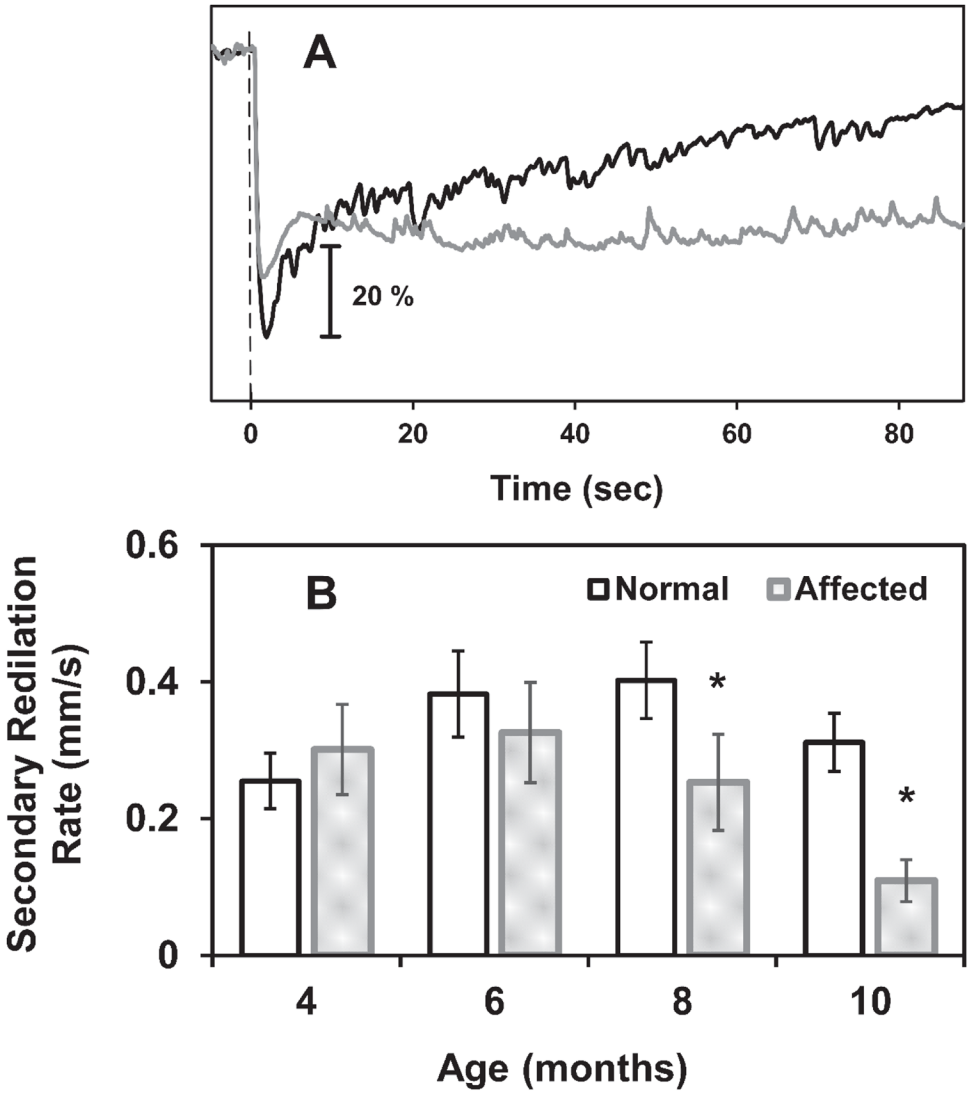

Figure 9.

The rate of secondary redilation is reduced in CLN2-affected dogs at 8 and 10 months of age. (A) Sample PLR traces from 10 month old dogs shown as percent of baseline pupil area using a 15 log photons/cm^2/s flash. The normal dog pupil gradually redilates to its baseline size (black plot) while the pupil from the affected dog maintains its constricted size for well over 85 seconds after light offset (gray plot). The vertical dashed line represents stimulus onset. (B) The rate of change in pupil diameter (mm/s) during secondary redilation, after a 15 log photons/cm^2/s flash, was decreased in 8 and 10 month old affected dogs (*, $p<0.025$) indicating that constriction persists longer after light offset.

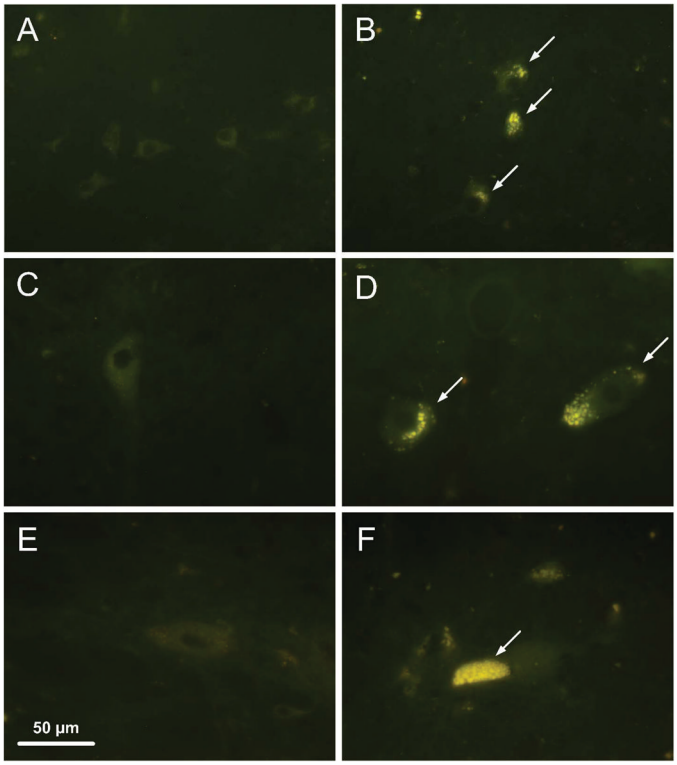

Figure 10.
Fluorescence micrographs of unstained cryostat sections of the pretectal nucleus (A, B), the parasympathetic region of the oculomotor nucleus (C,D), and the intermediolateral gray column of the cranial thoracic spinal cord (E,F) from 10 to 11 month old normal (A,C,E) and CLN2-affected (B,D,F) Dachshunds. Yellow-emitting autofluorescent storage material was present in the cell bodies of all 3 regions in the CLN2-affected dogs.